Hydrological and Climate Risk Assessment for the Cimanuk River Basin, Indonesia

September 2018

Author
R. van Tilburg

FutureWater Internship Report

FutureWater
Costerweg 1V
6702 AA Wageningen
The Netherlands

+31 (0)317 460050

info@futurewater.nl

www.futurewater.nl

Summary

In order to support Asian Development Banks's TA-9191 project a Climate Risk Assessment (CRA) is performed for the Cimanuk basin in Java (Indonesia). Many studies make a distinction between climate scenario driven impact assessment approaches, often referred to as "**top-down**". However, these top-down approaches start by downscaling Global Climate Model (GCM) projections and run these through (hydrological) models to develop projections for climate changes and is mostly used in climate scenario driven impact assessments. The major drawback of this method is, however, the limitation of the GCM projections. It takes a lot of time and effort to downscale these projections. Therefore a "**bottom-up**" approach is applied here which starts in the vulnerability domain. By the use of the rainfall-runoff model *SPHY,* multiple stress tests are applied to show the effect of changes in temperature and precipitation on multiple hydrological variables. Results show little effect of temperature, but a dominant effect of precipitation on the discharge. Combined with an ensemble of GCMs and RCPs for 2030, 2050, and 2100 it is shown that a large uncertainty is present for hydrological extremes as well as the average daily discharge. It is also shown that in terms of extreme discharge not only changes in temperature and mean precipitation, but also extreme precipitation events (99th percentile) changes should be considered. An inter-comparison between sub-basins showed the identical effects of climate change between a large and a small basin based on hydrology.

Table of contents

Tables

Figures

1 Introduction

1.1 Background

This study is part of the 2017 Asian Development Bank-TA project “Building Climate Resilience in Asia’s Critical Infrastructure” (TA-9191). The outcome of this project will enhance the knowledge based on climate risks to critical infrastructure in South Asia and Southeast Asia with focus on three countries (Indonesia, Sri Lanka, and Vietnam), in three sectors (water, transportation, and energy). This knowledge is then used to get a more complete understanding regarding what actions and innovations are needed to become more resilient to climate change.

This study focuses on the Cimanuk basin in Java. In 2016 a thorough study has been performed to grasp the water assessment in Indonesia (Asian Development Bank, 2016). This study shows the importance of understanding the water availability for future scenarios as the demand is rising due to population growth. Not only will this indicate a higher demand of water but also an enhanced demand of energy that needs to be generated by hydropower. This addresses the importance of understanding the hydrological processes including understanding the effect of climate change.

In order to support the TA-9191 project a Climate Risk Assessment (CRA) is performed. However, there is no standardized CRA methodology. Many studies make a distinction between climate scenario driven impact assessment approaches, often referred to as “**top-down**” (Burton et al., 2002; Carter et al., 1994; Wilby & Dessai, 2010). Top-down approaches begin by downscaling Global Climate Model (GCM) projections and run these through (hydrological) models to develop projections for climate changes and are mostly used in climate scenario driven impact assessments. The major drawback of this method is, however, the limitation of the GCM projections. It takes a lot of time and effort to downscale these projections. Therefore a “**bottom-up**” approach is suggested by García et al. (2014) which is used for vulnerability-oriented approaches. In contrast to the top-down approach, bottom-up approaches starts in the vulnerability domain (Figure 1). In practice this is done by adjusting forcing variables, simply altered by a range of possible future outcomes to indicate the effect of climate change on a certain output variable. Multiple forcing alterations are then combined in a map and on top of this GCM projections are plotted. This will give a clear overview of the impact of climate change on this output variable.

Using the rainfall-runoff model *SPHY* (Spatial Processes in Hydrology) in a bottom-up modeling approach, an impression of the effect of climate change on the hydrological processes for Cimanuk can be determined. SPHY is able to calculate the water balance and streamflow per (sub-)catchment. However it neglects anthropogenic influences such as water use and hydropower. Therefore, the results are used as input for an additional study using the water allocation/supply model WEAP (Water Evaluation And Planning System) to account for these lacking influences and to assess water availability.

1.2 Objectives

The objective of this research project is to understand and grasp the impact of climate change for hydrological processes in the Cimanuk catchment by the use of the SPHY rainfall-runoff model in a bottom-up modeling approach.

The main question to be answered is formulated by:

"What is the impact of climate change on the hydrological processes in the Cimanuk catchment?"

In order to answer this main research question the following sub-questions are identified:

1. What is the impact of temperature on discharge?
2. Will the climate projection of 2100, compared to 2030 and 2050, have the most impact on the discharge?
3. What is the impact of climate change on hydrological extremes?
4. Does the effect of climate change depend on the basin size?

1.3 Structure of report

The outline of this report is as follows. First, the study area (Cimanuk) is described in Chapter 2, followed by the description of the SPHY model in Chapter 3. The model set-up is thoroughly described in Chapter 4, followed by the methodology of the bottom-up approach in Chapter 5. In Chapter 6 the results are presented and finally in chapter 7 conclusion, discussion, and recommendations are presented.

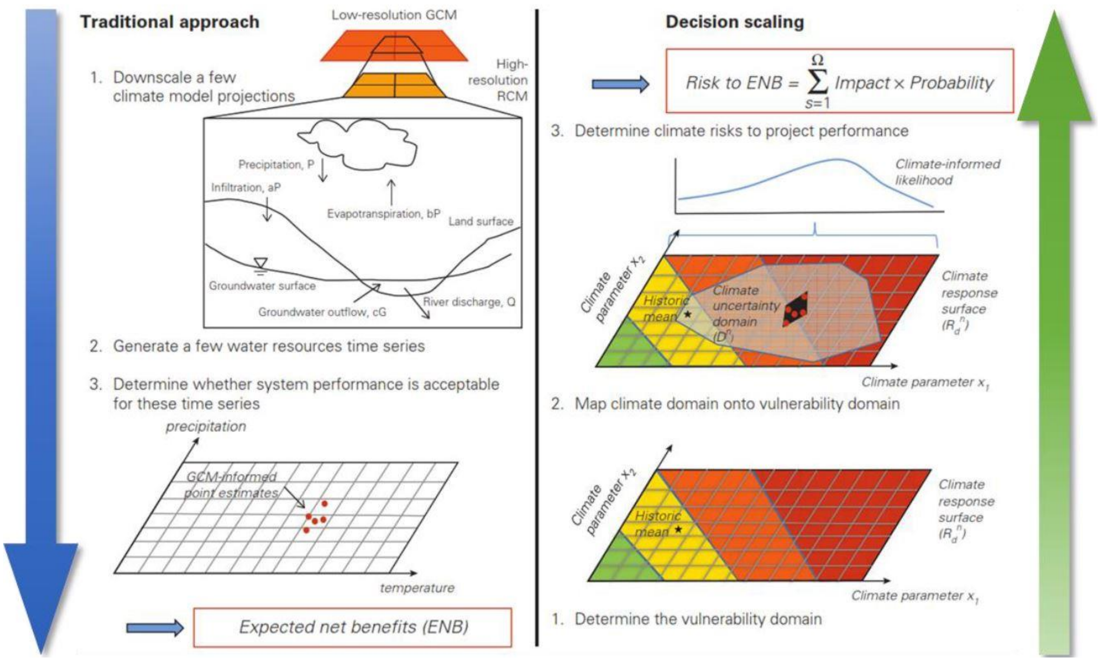

Figure 1 Top-down versus bottom-up risk assessment (García et al., 2014)

2 Study Area

2.1 General Description

The Cimanuk river basin is located in West Java, has a catchment area of 7,705 km^2 and is home to about 10 million people. The main river (Cimanuk) is 230 km long with a catchment area of 3,600 m^2 and is one of the largest rivers in West Java. Its origin is located on Mt. Papandayan (2,622 m) and Mandalagari (1,813 m), which are only 25 km away from the southern coast of Java. The upper basins is an elevated plateau at about 700 m, surrounded by multiple volcanoes. The lower basin consists of coastal plains below the elevation of 50 m. The climate is characterized by a wet season from October to April and a dry season from May to September. Water is mostly used for irrigation, with demand based on cropping patterns where rice is the main crop. In general this irrigation is applied from October to January and April to August with peaks in June and July.

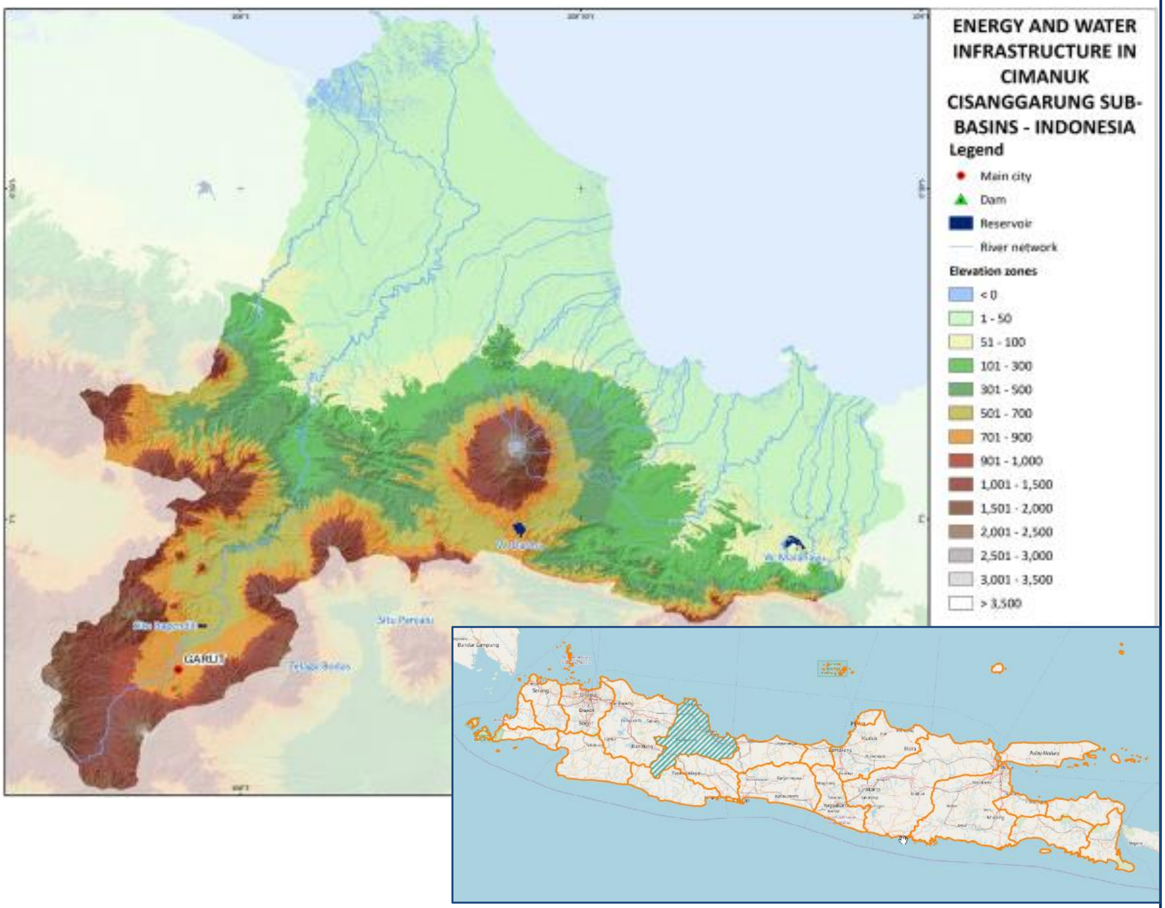

Figure 2 Altitude map of the Cimanuk river basin, including rivers and reservoirs. From: Global Reservoir and Dam (GRanD), v1.1 ICEM GIS Database.

2.2 Land use

The landuse in Cimanuk in mostly dominated by rice fields (35.99%), other crops (29.76%) and forests (22.76%), as can be seen in Figure 3. The forests are severely reduced during the 20th century. Agriculture is mainly irrigated rice and vegetables in the higher regions. Also tea and forest production is present. The major consumer of water is irrigation, mainly irrigated rice, with demand patterns based on the cropping patterns.

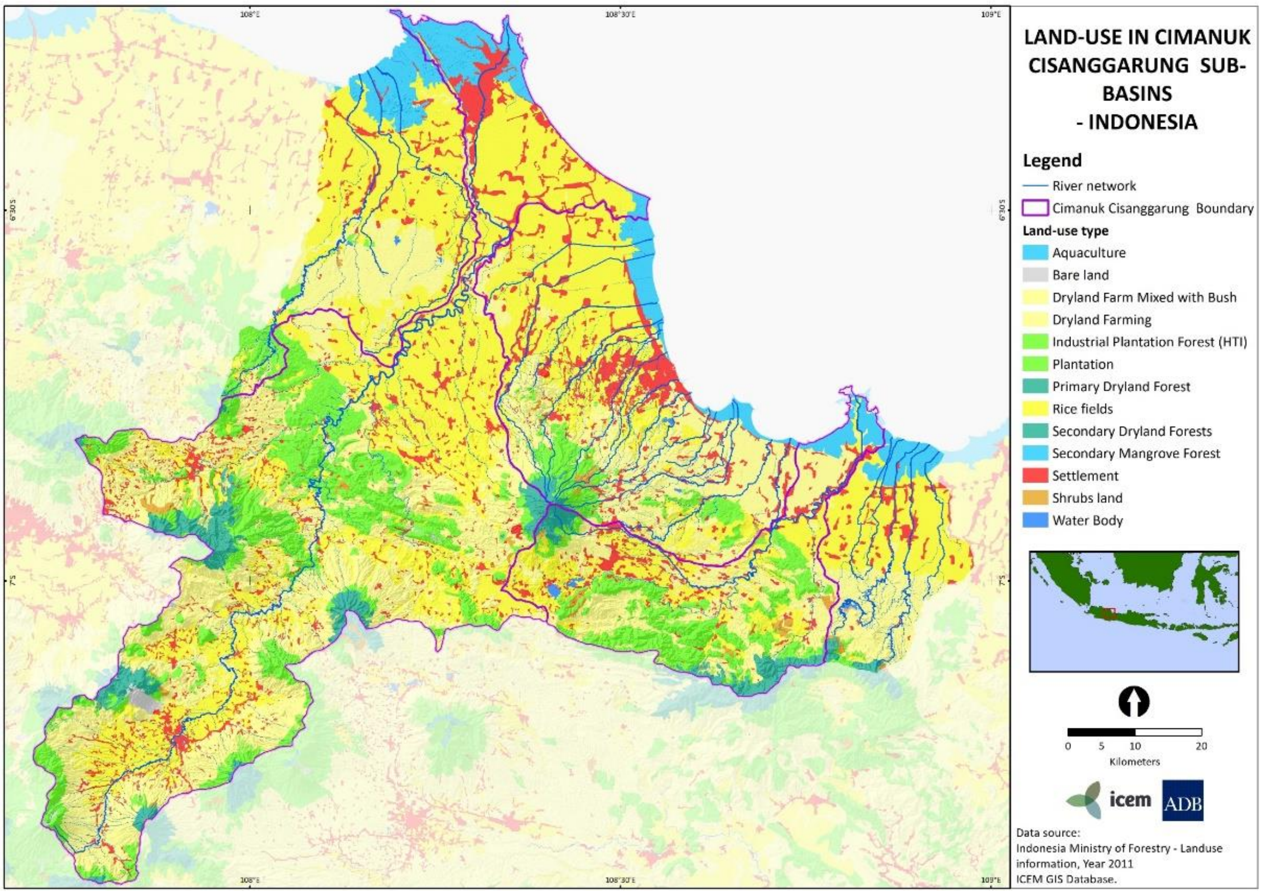

Figure 3 Land use map of the Cimanuk river basin, including rivers. From: Indonesia Ministry of Forestry – Landuse information, year 2010. ICEM GIS Database.

2.3 Climate

Precipitation is based on the annual movement of the inter-tropical convergence zone (ITCZ), that dictates a wet season from October to April and a dry season from May to September. Due to the presence of large uplifted areas, spatial precipitation patterns are correlated. In some areas, a yearly amount of 4000 mm is present compared to coastal areas with only 500 mm of precipitation yearly. Precipitation intensities of 30 mm/h are not uncommon, because of the tropical climate. The average temperature is around 26.5 °C – 28.5 °C. Even though the mountains are fairly high, no snow is present.

2.4 Sub-basins

The determination of sub-basins is based on the location of dams, reservoirs, and catchment boundaries. In Figure 4 all main rivers are shown, including the location of discharge stations available for model validation. The main river catchment is divided to multiple segments by dams and a reservoir. In this study the main focus is on the large Cimanuk catchment (Sub-basin 1,10,9, and 8). However, also an analysis will be performed on sub-basin number 3 to study the effect of basin size. In this basin the main river to be analyzed is the S. Cisanggarung, which has the same land use classes as the Cimanuk catchment. But the size of the basin is smaller.

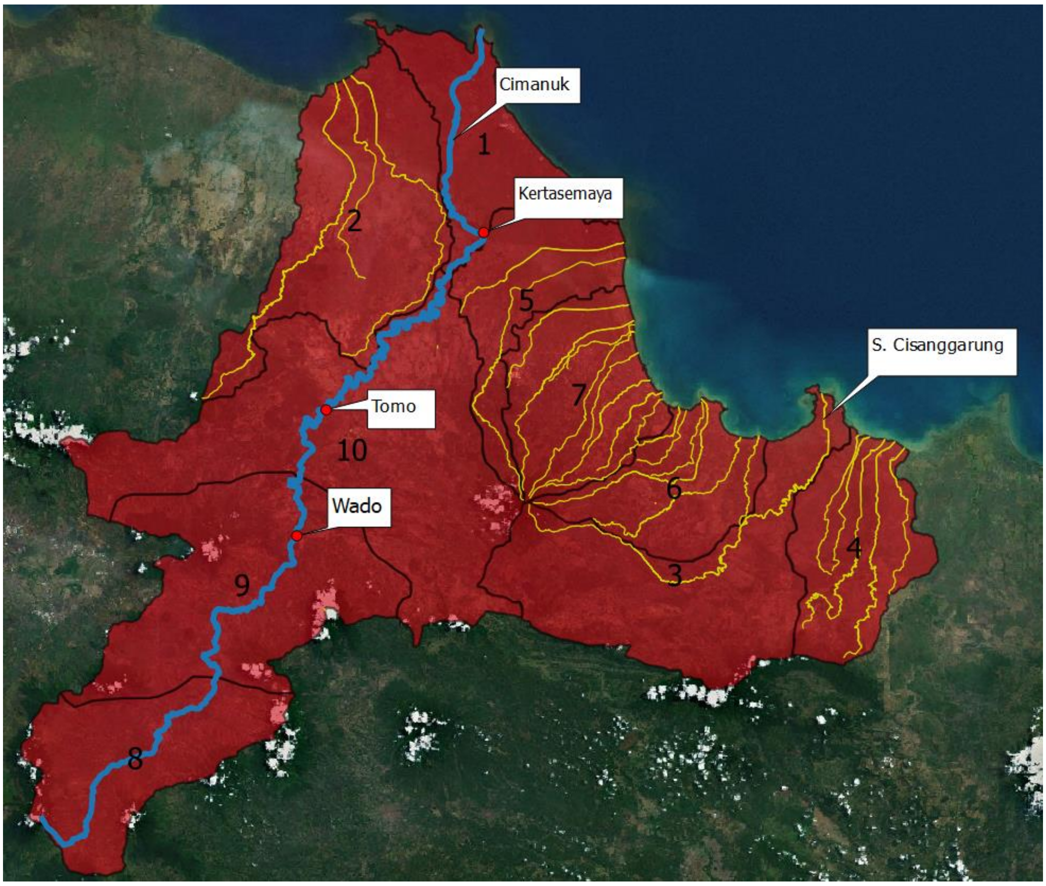

Figure 4 Sub-basins of the Cimanuk river basin based on dams, rivers, and reservoirs. Including the main rivers (Strahler order = 1), where the Cimanuk river is colored blue.

3 Model Description

The model that is used in this study is SPHY (Spatial Processes in Hydrology), developed by FutureWater. The aim of developing this model was to simulate terrestrial hydrology at multiple scales, with different land use and climate conditions, and under data-scarce conditions. It is a spatially distributed leaky bucket type model, applied on a cell-by-cell basis (Terink et al., 2015). As energy-balance calculations require high-resolution data, e.g. using the Penman-Monteith equation, this will result in more parameters and therefore larger computation times (Allen et al., 1998). SPHY therefore neglects any energy-balance computations defining itself as a water-balance based model. The SPHY model is written in the Python programming language and makes use of PCRaster dynamic modelling framework (Karssenberg et al., 2001). The version used in this internship report is SPHY2.2, which is freely available[1].

In Figure 5 an overview of all concepts are shown. SPHY is grid-based and sub-grid variability is possible for glaciation, i.e. a cell can be glacier-free, partially glacierized, or completely covered by glaciers. Land that is free of snow can consist of vegetation, bare soil, or open water. The soil structure consists of two upper soil reservoirs (rootzone and subzone) and an underlying groundwater reservoir. Drainage from these reservoirs occurs in the form of three flow components: surface runoff, lateral flow, and baseflow. The sum of these components is called the cell-specific runoff. Precipitation is simulated per cell as snow or rain, depending on the temperature. Precipitation can be intercepted by vegetation and eventually evaporated. Depending on the area of interest multiple modules can be turned on or off. The available modules are: glaciers, snow, groundwater, dynamic vegetation, simple routing, and lake/reservoir routing. All these modules can be used independently from each other, except the glacier module. Any non-relevant modules should be turned off to reduce computational times and input data needed. In this study the only relevant modules used are groundwater and simple routing. More details regarding these modules can be found in Terink et al. (2015).

[1] https://github.com/FutureWater/SPHY

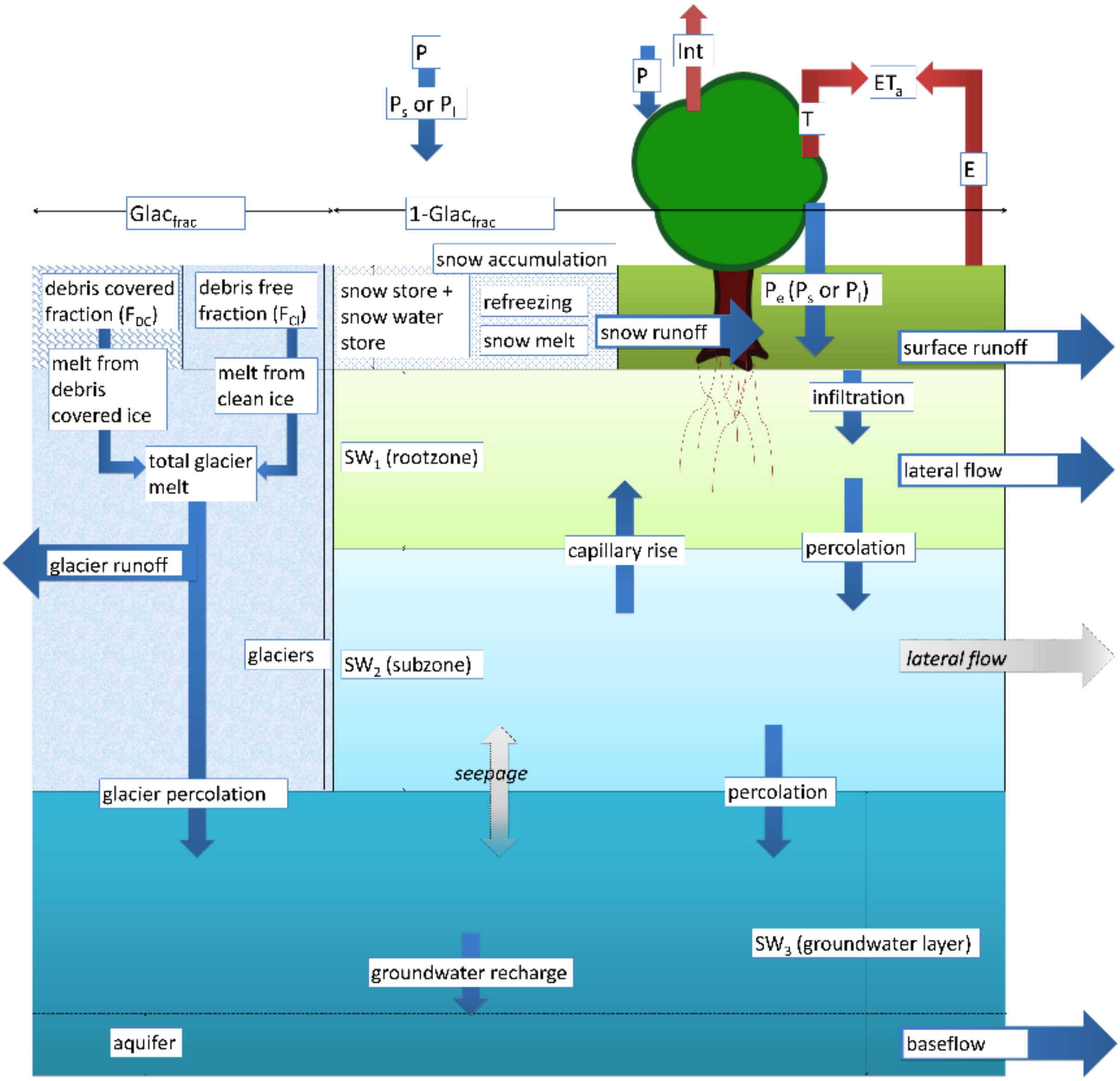

Figure 5 SPHY model structure, copied from Terink et al. (2015).

4 Model Set-up

In this section the creation of input data/maps needed for SPHY is explained. SPHY needs static as well as dynamic data/maps as input. Static maps that are used are: DEM (Digital Elevation Model), land use type, soil characteristics, stations, latitude, clone, accuflux, and Local Drain Direction (LDD). Dynamic data is meteorological forcing such as precipitation, temperature and reference evapotranspiration. As SPHY is grid based, all input maps should have the same resolution and extent. In order to limit computation times and preserve realistic grid resolution, the resolution of the raster maps is determined to be 500x500 m with a temporal resolution of a day. To capture the whole catchment the extent of the raster is based on 293x271 cells, which are almost 80.000 cells. The data period is selected to be 1995-2015, this is based on the quality and availability of the forcing data.

4.1 Static input data

4.1.1 Digital Elevation Model and Local Drain Direction

The first map to be created was the DEM, which indicates the surface height of the study area above sea level. The DEM is obtained from HydroSHEDS (Hydrological data and maps based on SHuttle Elevation Derivatives at multiple Scales) (Lehner et al., 2006). However, the resolution of this DEM is based on 15 arc-seconds, which is near the equator already nearly equal to a 500 meter resolution. Therefore a small resampling is needed to fit the initial raster setting of 500x500 m. In Figure 2 the DEM is shown together with the location of the main rivers. It is clearly visible that the streams originate in the higher parts of the basin corresponding to the located volcanoes. From this DEM SPHY will calculate a local drain direction map (LDD) and a slope map, which are maps containing the flow direction and the slope respectively. Without any anthropogenic effect or complex geology, rivers will follow the natural direction, which is from higher to lower cells. In reality the pattern of rivers might be altered, for example in urbanized areas or due to the construction of a dam.

Based on the DEM, the LDD will generate a river network following the natural slope. In SPHY/PCraster streams never diverge, only convergence occurs. Areas containing a very gentle slope might result in small errors and cause divergent drain directions. In the study area, the coastal part is such an area. Therefore, solely using the DEM to calculate the LDD would lead to unrealistic draining networks. A method called stream burning has been used in this study to force the LDD to follow the 'real' rivers. The method is to first calculate a map with relative height values, ranging from 0 to 1. Then on top of this map, the main rivers (stream order 1, following the method of Hack (1957)) are plotted and provided with a value that will be subtracted from the relative height map to generate a stream burn map. Calculating the LDD from this map will result in flow directions corresponding to the real rivers.

4.1.2 Latitude map for evapotranspiration

In order to calculate reference evapotranspiration (ET_r [mm]), SPHY is using the modified Hargreaves method (Droogers & Allen, 2002). This method is applicable by knowing very little meteorological variables and therefore very useful in many regions of the world where data is scarce. The formula is implemented in SPHY according to:

$$\boldsymbol{ET_r = 0.0023 \cdot 0.408 \cdot RA\left(T_{avg} + 17.8\right) \cdot TD^{0.5}} \qquad \text{Eq.1}$$

with RA [$Mjm^{-2}d^{-1}$] the extraterrestrial radiation, T_{avg} [°C] the average daily air temperature, and TD [°C] the temperature range, defined as the difference between the daily maximum and minimum air temperature. Based on the day of year and the latitude per raster cell, the *RA* will be calculated by SPHY. This latitude per raster cell should be provided by a latitude map.

4.1.3 Land use and Kc-factors

The potential evapotranspiration can be calculated by using crop coefficients (Kc-factors) multiplied with ET_r, which is suggested by Allen et al. (1998). The formula is then defined as:

$$\boldsymbol{ET_{p,t} = ET_{r,t} \cdot Kc} \qquad \text{Eq.2}$$

This will give the daily ET_p. SPHY will calculate this based on a land use map in combination with coupled crop coefficient factors. The land cover map is shown in Figure 3. Every land cover type has been granted a crop factor based on Allen et al. (1998).

Table 1 Crop coefficients per land use type based on Allen et al. (1998)

Crop Type	*KC based on Allen et al. (1998)*
Aquaculture	1.05
Bare land	0.5
Dryland farm mixed with bush	0.9
Dryland farming	0.9
Industr. Plant. Forest	1.05
Plantation	1.2
Prim. Dryland forest	1.05
Rice fields	1.2
Sec. Dryland Forest	1.05
Secondary Mangrove Forest	1.1
Settlement	0.7
Shrubs	0.8
Water Body	0.85

4.1.4 Station locations

A station map with locations where output should be generated is needed. This map is based on strategic locations in order to analyze the whole catchment. First of all, it includes all outlets of all major streams at the coast, validation points, and points indicating the border of a sub-catchment.

4.1.5 Soil hydraulic properties

As SPHY uses a groundwater module, input regarding soil characteristics is required. The physical maps needed are:

- Field capacity
- Saturated water content
- Saturated hydraulic conductivity
- Permanent wilting point
- Wilting point

These five maps are needed for the rootzone, while only the first three mentioned are needed for the subzone. These maps are used in SPHY to calculate multiple hydrological processes, such as lateral flow, surface runoff, percolation, capillary rise, and evapotranspiration. In order to generate these maps, soil type maps are combined with the hydraulic soil properties stored in HiHydroSoil (de Boer, 2016). The polygons from the soil maps are used as masks over the data from HiHydroSoil and the median values of all parameters are then used as values for these areas.

4.1.6 Dynamic input data

One of the most import input maps is the meteorological forcing data. This data has to have the same temporal resolution as the model (day) and the same spatial raster resolution (500 x 500 m). The meteorological variables needed are T_{avg}, $T_{min,}$, $T_{max,}$ and precipitation.

Precipitation data is obtained from CHIRPS, which is a dataset based on interpolation and long period of precipitation records based on infrared Cold Cloud Duration (CCD) (Funk et al., 2015). This dataset has a spatial resolution of 0.05°(~5.5 km) and is globally distributed. The data period is from 1981 – PRESENT and is freely available. Beck et al. (2017) has evaluated the quality of CHIRPS with a comprehensive evaluation of rain gauges and noticed that the usage of CHIRPS is viable in tropical regions.

Temperature data (T_{avg}, $T_{min,}$, T_{max}) is obtained from WFDEI (WATCH Forcing data methodology applied to ERA-Interim reanalysis data) (Weedon et al., 2014). This data has a spatial resolution of 0.5°, meaning that local elevations are neglected. Therefore, this dataset is first downscaled to the same resolution of the DEM. By knowing the altitude per grid and applying a lapse rate formula in combination with the temperature data from WFDEI, a more accurate map can be produced. The lapse rate constant used is 0.0065 [°C m^{-1}], so multiplying this factor with elevation data from the DEM will result in a spatially downscaled map with temperature data.

4.2 Validation data

Validation data is required in order to calibrate SPHY. Unfortunately, very little validation data was provided for this study. A few data sets were available and used and are described below.

4.2.1 Precipitation data

Meteorological data was provided for a few stations in west and central Java. Unfortunately, only one station was actually located in the study area. This station, named "*Stasiun Meteorologi Jatiwangi*", is located on (108°16, -6°45; Figure 6) and measured daily basic meteorological variables (e.g. temperature, windspeed, precipitation) from 1988 until present. With this data the use of CHIRPS can be validated.

Figure 6 Meteorological station location of "*Stasiun Meteorologi Jatiwangi*". *From:* *http://epsg.io/*

4.2.2 Actual evapotranspiration ensemble product

The actual evapotranspiration (*ETa* [mm]) is calculated by multiplying *ETp* with reduction parameters and is generated as output in SPHY ($ET_{a,t} = ET_{p,t} \cdot ETred_{wet} \cdot ETred_{dry}$ Eq.3). This can be validated by the use of the ETa ensemble product developed by IHE[1]. This ensemble product is based on multiple remote sensing products based on 7 ET products:

- ALEXI (Mecikalski et al., 1999)
- CMRSET (Guerschman et al., 2009)
- MOD16 (Mu et al., 2007, 2011)
- SEBS (Su, 2002)
- SSEBop (Senay et al., 2007)
- ETmonitor (Hu & Jia, 2015)
- GLEAM (Martens et al., 2017)

[1] https://www.un-ihe.org/

For every pixel outliers are removed until the covariance is high enough. Afterwards the product is downscaled to a pixel size of 250 meters. The temporal scale was monthly from 2003 until 2014. The final product provided was uniquely for the Cimanuk basin.

4.2.3 Discharge data

Discharge data provided was available for multiple main rivers in Indonesia with annual discharge averages. However, for the Cimanuk river, only four measurement locations are present: Wado, Tomo, and Kertasemaja. Wado and Tomo corresponds to up and midstream areas respectively. Where Kertasemaja is located in the downstream part of the river basin (Figure 4). The data consist only of annual average discharges with just a few years covered. Kertasemaja had data from 2005 – 2010, while Wado and Tomo ranged from 2000 – 2010 with 2003 and 2004 lacking. As SPHY does not incorporate any water use based on anthropogenic situations (e.g. irrigation, consumption), data from mid/downstream will be neglected. Therefore, only data from Wado will be used for validation.

4.3 Calibration and Validation

In this study, a three-step approach was used: first the precipitation data was validated to rain gauge data, followed by the output of the model to match the ET product of IHE and thirdly the model was validated to match the provided mean annual river discharge.

4.3.1 CHIRPS validation

Comparing CHIRPS with the measured precipitation from *Stasiun Meteorologi Jatiwangi*, shows a very good correlation. This indicates that the use of CHIRPS in this study is valid (Figure 7). However, this does not guarantee the performance on other locations in the basin. Also, this indicates the validity of the monthly averaged per day. Though smaller temporal scales are not shown here, as they are not relevant for this study.

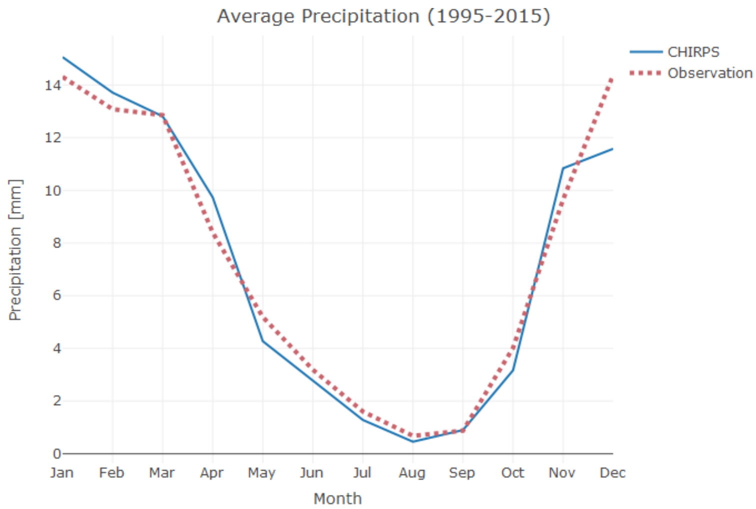

Figure 7 CHIRPS validation, based on the monthly averaged precipitation per day between 1995-2015.

4.3.2 Calibration to actual evapotranspiration

Due to the availability of monthly ETa data, calibration of this variable in SPHY is possible and is performed first. In order to calibrate this variable we need to understand the calculation of ETa per cell per timestep. In SPHY the formula for calculation of ETa per timestep is defined as:

$$ET_{a,t} = ET_{p,t} \cdot ETred_{wet} \cdot ETred_{dry} \quad \text{Eq.3}$$

with $ET_{a,t}$ [mm] the actual evapotranspiration on day t, $ET_{p,t}$ [mm] the potential evapotranspiration on day t, and $ETred_{wet}$ and $ETred_{dry}$ reduction parameters for water excess and water shortage conditions, respectively. In reality there are many more limiting factors (e.g. salinity stress, diseases), however since SPHY is a water-balance model only these two reduction parameters are taken into account. $ETred_{wet}$ is a value in SPHY that is either 0 (saturated soil) or 1 (non-saturated). As the soil is saturated, the plant is unable to extract any water due to oxygen stress (Bartholomeus et al., 2008). However, this is not valid for every crop type (e.g. rice). $ETred_{dry}$ indicates the shortage of water, calculated by the Feddes equation (Feddes, 1978).

The calculation of ET_a is thus based on several variables, where most of these are based on soil characteristics ($ETred_{wet}$ and $ETred_{dry}$) or meteorological forcing (ET_p). This leaves Kc-factors to be the key parameter to calibrate, because they can be quite uncertain. To do so, every land use type of the land use map will be combined with the given ETa product to calculate the monthly ETa per land use type.

In Figure 8 the dominant crop type (rice) is shown for the uncalibrated (SPHY Raw) and calibrated Kc-factor (SPHY). The red dots indicate low ET_a values, though these periods should indicate large amounts of ET_a compared with IHE ET_a product. The large reduction of ET_a is caused by the $ETred_{wet}$ parameter that during periods of excessive precipitation has a value of 0. This is not realistic and therefore the parameter is permanently set to 1, to avoid this phenomenon. Afterwards, the Kc-factor is altered in such a way that the mean of the calculated ET_a is as close as possible to the measured ET_a. The mean is taken here, because this study is interested in the water balance subject to climate change and therefore the long-term water balance should be in order. To check this, cumulative evapotranspiration is compared for simulated and measured and the cumulative deficit is calculated and shown with the Kc-factors together in Table 2.

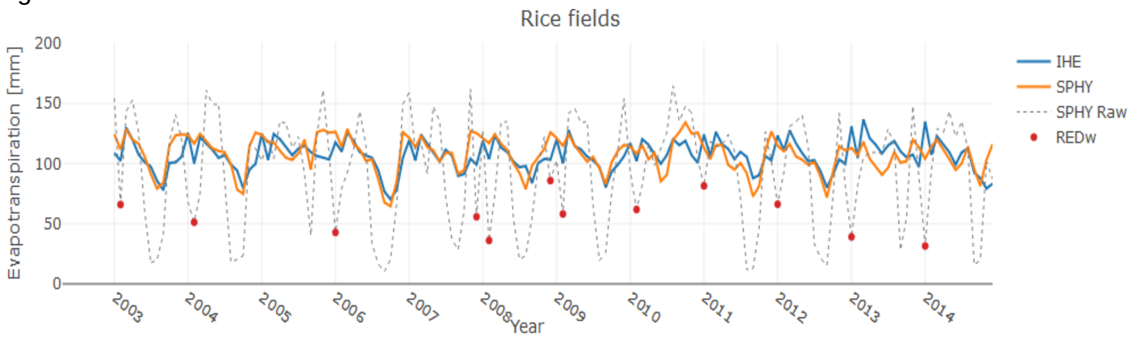

Figure 8 Evapotranspiration of rice field, validated against the IHE ensembleET data set. Including the uncalibrated, calibrated graph, and the effect of the REDw parameter.

Table 2 New and old crop factors and cumulative deficit of the dominant land use class.

Crop Type	*Old Kc*	*New Kc*	*% cumulative deficit*
Rice field	1.2	0.84	1.2
Forest	1.05	0.9	1.8
Crops	0.9	0.83	1.8

4.3.3 Discharge validation

P and ETa are now validated, however the most important variables to be validated yet is discharge. Unfortunately, the data provided is only the annual mean discharge and for just a few years. In Cimanuk, a lot of water is used for irrigation or consumption, which is not taken into account in SPHY, and therefore only data from upstream regions can be used. Wado is therefore the only useful station due to the upstream location. Comparing observed discharge at this station with output of SPHY shows, surprisingly, a few years with a lot of deviation. In order to test the observational data a hypothetical discharge is introduced here. This discharge is calculated by the use of CHIRPS and the ET product of IHE. Subtracting ET from CHIRPS results in discharge, based on a simple water balance. This is performed at the same location of the observation. Figure 9 shows the hypothetical, modelled, and measured discharge. This figure shows still a large deviation from the observations, but is relatively close to the results of SPHY. Also, there is no significant trend in the deviations between observations and output. In other words, the difference between observed and modelled discharge are rather non-systematic and therefore unable to use for proper calibration. Therefore, the decision has been made to neglect this data set and only calibrate the model on actual evapotranspiration.

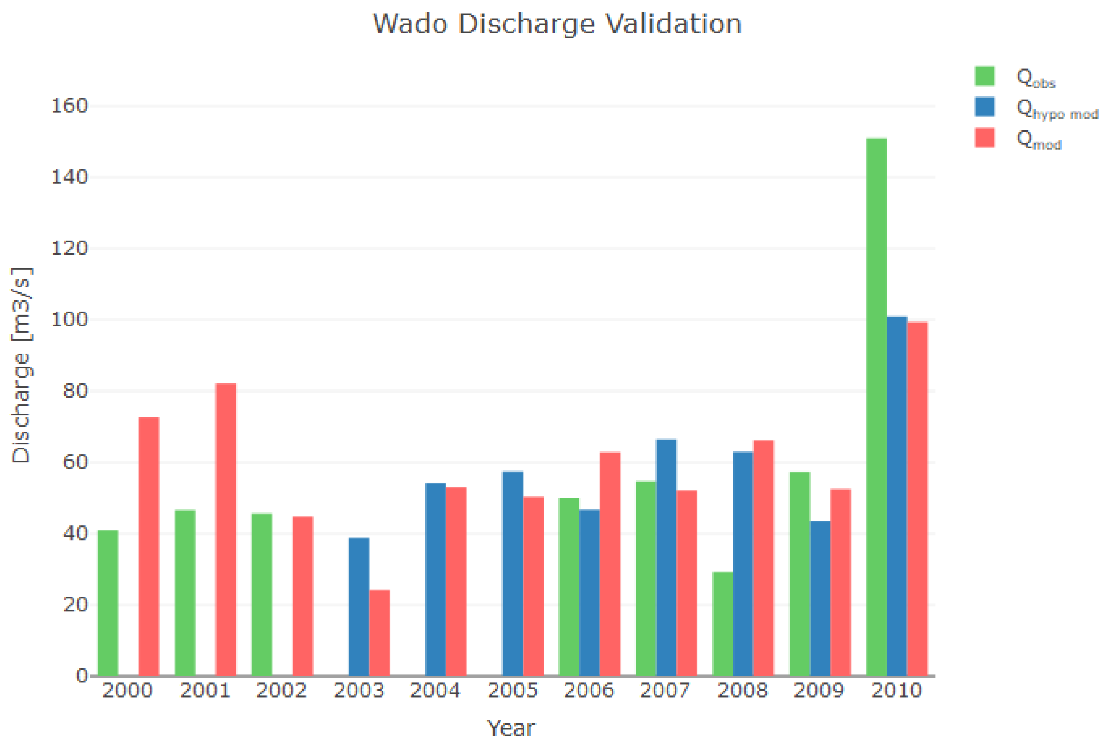

Figure 9 Wado discharge validation, including a hypothetical discharge.

4.4 Spin-up period

As limited data is available, initial conditions are hard to determine. In order to improve the quality of the model run and get better results a spin-up period is implemented in the model. This spin-up period will run for two years, so that certain initial conditions (e.g. groundwater level, discharge) are better defined then by just iterating. In other words, this is to ensure different reservoirs in the model reach realistic levels. The methodology to implement such a spin-up period is quite simple. In this study we copied the first two years of forcing and pasted it in front of the existing forcing.

5 Bottom-up approach

In order to explain future scenarios, a bottom up approach will be performed. To start, a stress test is applied by selecting a range of different combinations of precipitation and temperature indicators to transform to future possibilities. Afterwards, Global Climate Models (GCMs) are selected and used together with the outcome of the stress test. This is called the 'Bottom-up' approach. In this chapter the methodology of such a 'Bottom-up' approach is described.

5.1 Stress Test

The stress test is first based on two variables: temperature and precipitation. Conversion of these variables is easily applied in the following way. Temperature data is altered by adding a range of degrees starting from zero to eight to the whole forcing data set equally. This results in nine altered temperature data sets. The same method is applied for precipitation, however instead of adding an integer the whole data set is multiplied with factors ranging from 0.6 to 1.4. In other words, the precipitation data set has decreasing or increasing precipitation amounts varying with 40%. However, this method of changing the entire distribution of a variable is valid to use for temperature in this study, but precipitation has a more complex behavior in future scenarios. This study aims to assess the effect of future changes in precipitation extremes for hydrological extremes as well. Not only will there be more extremes, also mean precipitation amounts will be different and therefore Shabalova et al. (2003) suggested a formula to transform observed precipitation towards a future scenario based on the results of GCM data. However, applying this formula will result sometimes in negative precipitation values. Therefore we will use the same formula as Leander and Buishand (2007), which is based on applying the Weibull distribution on the method of Shabalova et al. (2003). This formula is transforming precipitation (P) to a corrected precipitation (P*) by the use of an *a* and *b* coefficient :

$$\boldsymbol{P^* = aP^b} \qquad \text{Eq.4}$$

By determining different mean and P_{99} multiplication factors, where P_{99} stands for the 99th percentile of precipitation, *a* and *b* coefficients will be calculated based on minimizing the sum of squares of the mean and P_{99} per cell over all timesteps. These alterations of mean and P_{99} are based on the same factors used before, thus ranging from 0.6 to 1.4. This method has to be applied to all 80,000 cells resulting in two maps per combination with *a* and *b* values for every

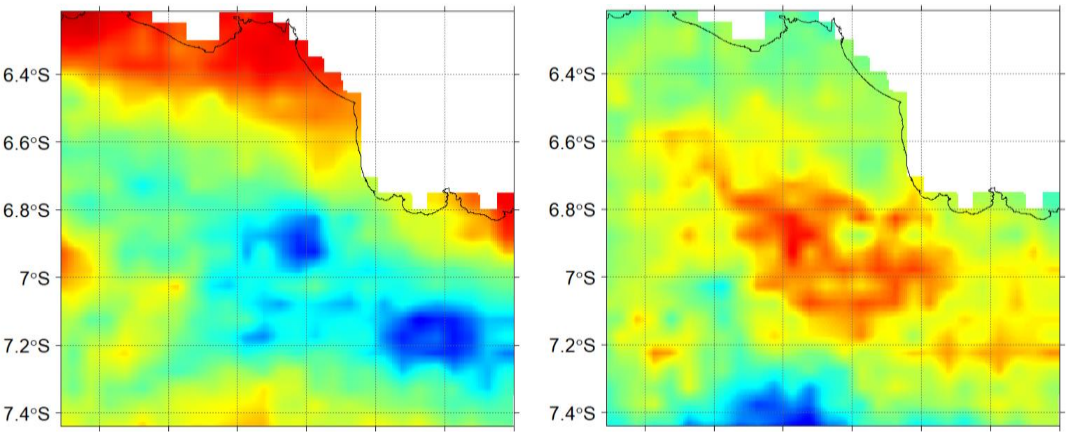

Figure 10 Example of an a (left) and b(right) coefficient map for the combination of $P_{mean,120}$ and $P_{99,60}$

cell. In Figure 10 such coefficient maps are shown for the combination $P_{mean,120}$ and $P_{99,60}$, thus an increase of 20% for the mean precipitation with a decrease of 40% for P_{99}.

5.2 Climate change scenarios

In the fifth Assessment Report from the Intergovernmental Panel on Climate Change, four representative concentration pathways (RCPs) have been defined for long-term and near-term modeling experiments (van Vuuren et al., 2011). Based on open literature, these four pathways span the range of year 2100 radiative forcing values ranging from 2.6 to 8.5 W/m^2. These four pathways are used by climate modelers for their climate modelling experiments to simulate climate scenarios. As pointed out by Moss et al. (2010) the community needs new scenarios. Based on these RCPs it allows climate modelling experiments parallel to the development of emission and socio-economic scenarios.

Based on the four RCPs multiple GCM's are used for the Cimanuk basin. The GCMs are using the same reference period as our study period and based on this, the change in *P* and *T* can be determined for different future scenarios. This study is interested in the climate change for the years 2030, 2050, and 2100. Therefore, the relevant output of these GCMs will be 2021-2040, 2041-2060, and 2081-2100 respectively. Based on all values for delta *P* and delta *T*, combined with the outcome of the stress test will give a solid understanding of the effects of climate change in the Cimanuk basin for different hydrological properties, and the likeliness of their occurrence in the future.

Table 3 Description and visualization of the four representative concentration pathways (RCPs) (van Vuuren et al., 2011)

RCP	Description
RCP8.5	Rising radiative forcing pathway leading to 8.5 W/m^2 (~1370 ppm CO_2eq) by 2100
RCP6	Stabilization without overshoot pathway to 6 W/m^2 (~850 ppm CO_2eq) at stabilization after 2100
RCP4.5	Stabilization without overshoot pathway to W/m^2 (~650 ppm CO_2eq) at stabilization after 2100
RCP2.6	Peak in radiative forcing at ~3 W/m^2 (~490 ppm CO_2eq) before 2100 and then decline (the selected pathway declines to 2.6 Wm2 by 2100

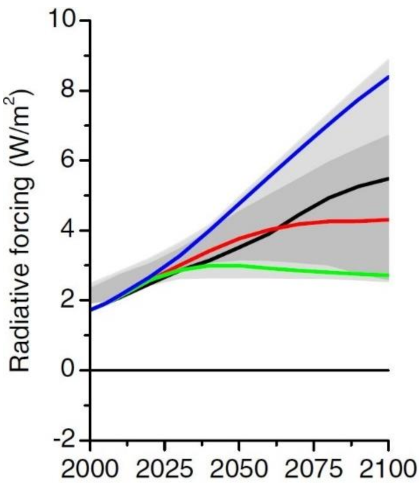

Figure 11 RCPs. Blue: RCP8.5, black: RCP6, red: RCP4.5, green: RCP2.6 (van Vuuren et al., 2011)

6 Results

In this chapter the results are shown, starting with the discharges of the main river compared to S. Cisanggarung. First basic hydrologic properties are described, followed by the effect of climate change on these rivers.

6.1 Present situation

6.1.1 Cimanuk River

After calibration and adding spin-up time, SPHY is able to generate discharge output at any point of the catchment as long as this point is equal to the size of the resolution. In Figure 12 the discharge pattern is shown for the outlet of the Cimanuk river. The seasonality is clearly visible, with dry periods ranging from August-October. During the study period of 21 years, the average daily discharge per month can be as high as 500 m^3/s or as low as 0.25 m^3/s. In Table 4 other hydrological properties are calculated, such as the average discharge, maximum discharge, and average of days that are below the 5th percentile taking 1995-2015 as reference period.

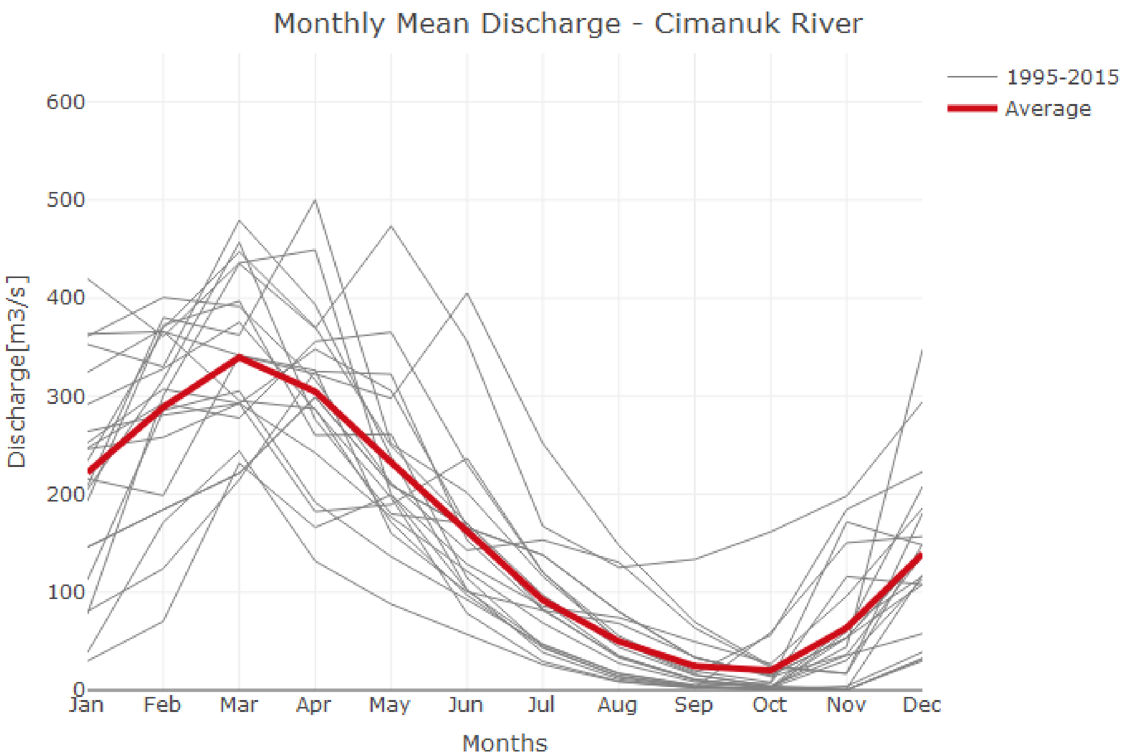

Figure 12 Monthly mean simulated discharge of the Cimanuk river from 1995-2015. Red line indicates the mean discharge.

Table 4 Simulated hydrological properties of Cimanuk and S.Cisanggarung river in the Cimanuk basin, based on period 1995-2015.

Variable	*Cimanuk*	*S.Cisanggarung*
Average [m^3/s]	161	53.1
Max. Discharge [m^3/s]	654	190.3
Average days < 5th percentile [days]	18.3	18.3

6.1.2 S. Cisanggarung

The S. Cisanggarung river has more or less the same seasonal pattern as the Cimanuk River. However, it is clearly visible that the lines are steeper, because this sub-catchment is much smaller than the Cimanuk sub-catchment. Also the distance from origin to the outlet is smaller. This indicates lower storage capacity and therefore a higher rainfall runoff rate. This will therefore result in higher peaks, lower lows, and larger changes in mean discharge.

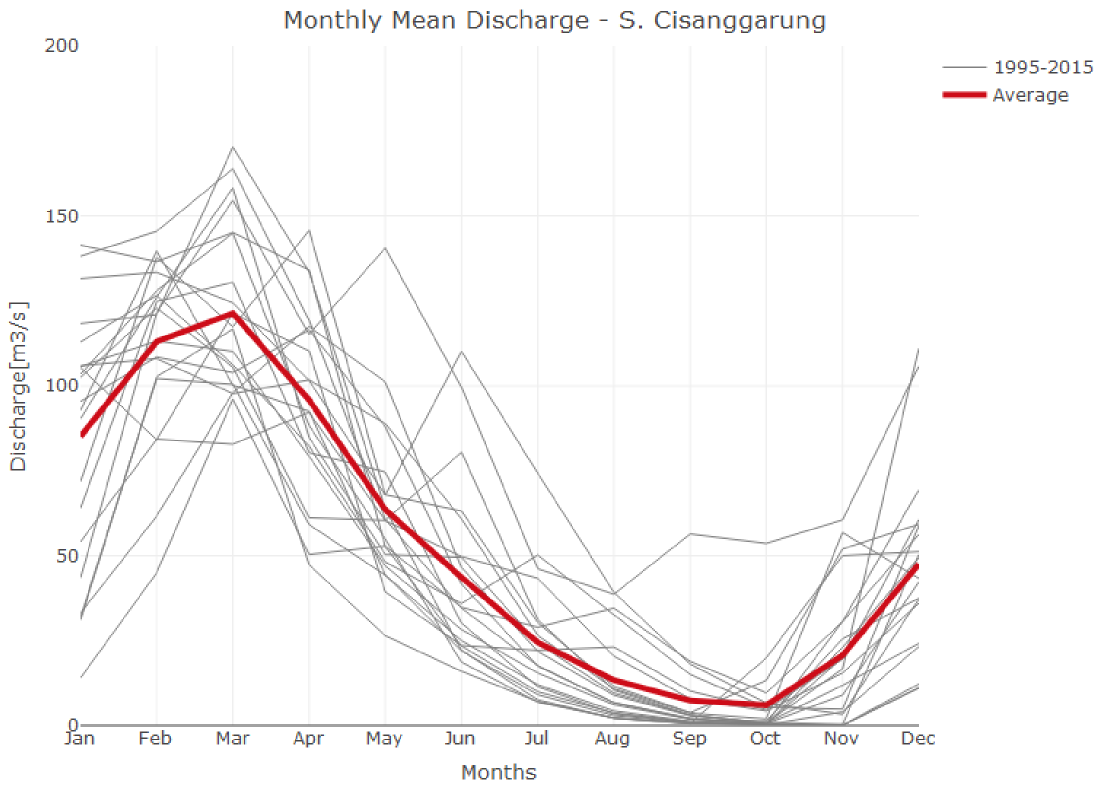

Figure 13 Monthly mean simulated discharge of the Cimanuk river from 1995-2015. Red line indicates the mean discharge.

6.2 Cimanuk river

6.2.1 Average daily discharge

In Figure 14 the results of the first stress tests are shown. These tests indicate the effect of climate change on the daily discharge of the main Cimanuk river. It is clearly visible that the effect of rising temperature barely has any effect on the streamflow. This indicates that the amount of evapotranspiration is less important than the run-off component generated by increasing precipitation. The reference daily discharge is 161 m^3/s, as shown in Table 4. Based on this value it shows that for our stress test, the discharge can rise by 180% if the mean precipitation would increase by 140% while temperature doesn't change at all. Or the discharge can also decrease to 20% by a combination of the highest temperature increase with the highest decrease in precipitation amounts. This indicates a large spread of possibilities and extra information is needed to assess climate change effects

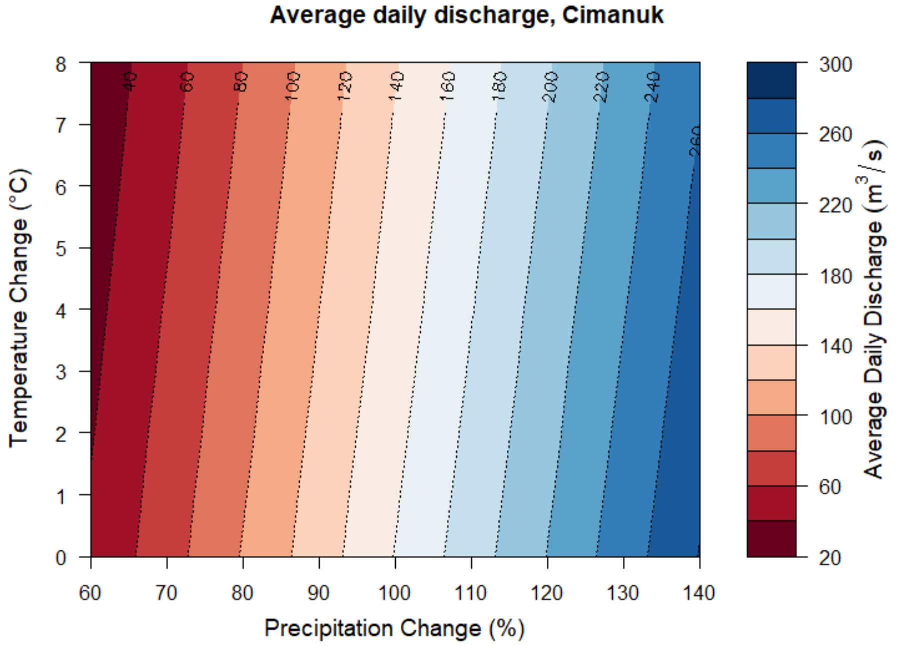

Figure 14 Stress test of the average daily discharge in the Cimanuk river, based on average changes in temperature and precipitation.

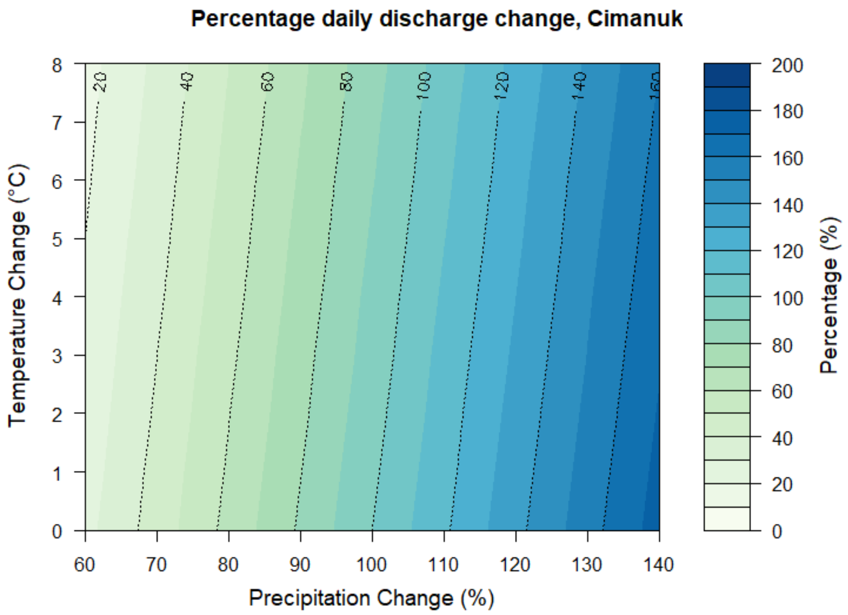

Figure 15 Percental change of average daily discharge in the Cimanuk river, based on stress test with changes in average temperature and precipitation.

6.2.2 Hydrological Extremes

In terms of extremes, we analyzed low flows and extremely high discharges. Low flows are defined as the discharge value under the 5^{th} percentile of the reference period (1995-2015). We show the average number of days annually that discharge is under this value. This information is key to understanding future drought scenarios in terms of water availability. As irrigation is very important, low discharge days can be crucial to the crops and vegetation. In Figure 16 the same procedure is performed as shown earlier, but now for the average number of days below the 5^{th} percentile threshold. Again, the impact of precipitation on this variable is clearly visible.

Here increasing precipitation patterns will, obviously, decrease the number of days below the threshold and decreasing precipitation patterns will enhance it. However, for low discharges temperature does play a more important role compared to its role for overall water availability. Especially with higher precipitation amounts in combination with higher temperatures will result in more dryer days.

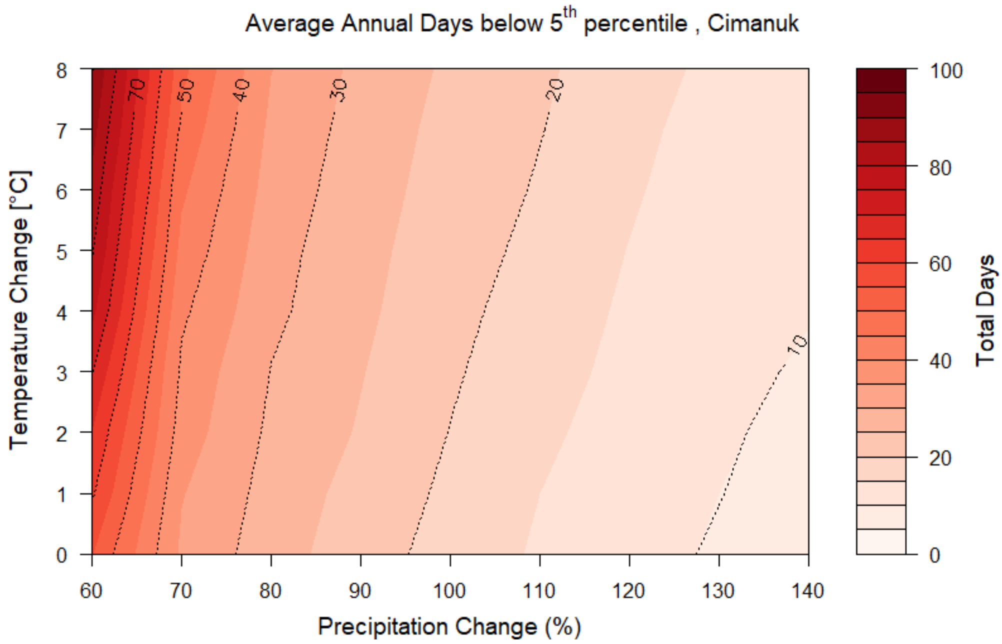

Figure 16 Stress test of the average annual days below the 5th percentile of discharge in the Cimanuk river, based on changes in temperature and precipitation

For the maximum discharge (Figure 17), the same pattern is shown again as seen before where the impact of temperature is less dominant than precipitation. However the increase of the maximum discharge is notable. Under current conditions the maximum daily discharge is as high as 654 m^3/s. The stress test shows us that under the most extreme conditions it can become as high as 950 m^3/s, which is really significant.

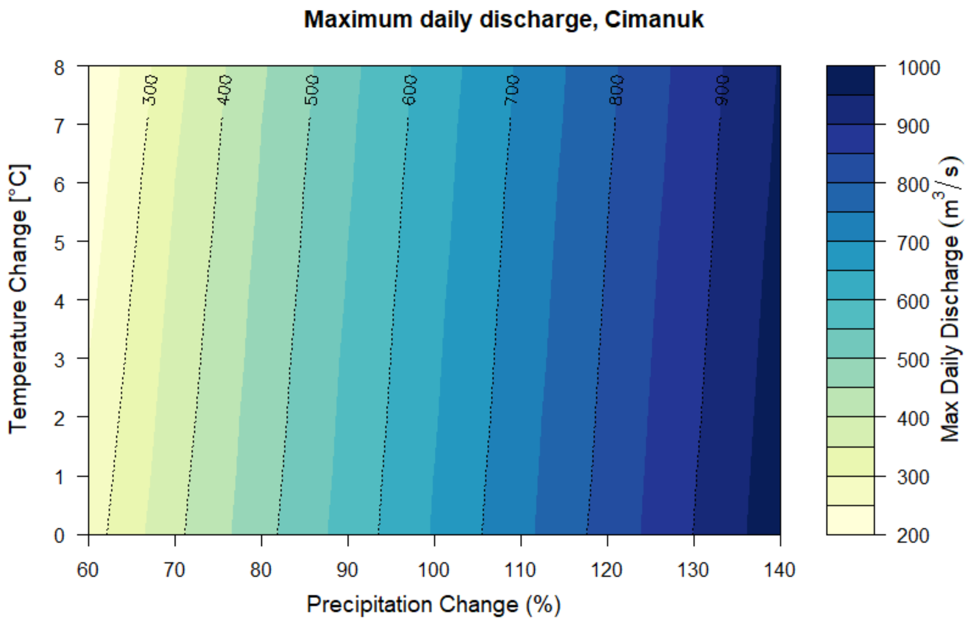

Figure 17 Stress test of the maximum daily discharge in the Cimanuk river, based on changes in temperature and precipitation.

As not only the mean precipitation amounts change due to climate change, we also did a stress test regarding a change in P_{99} (99th percentile of precipitation) and the P_{mean}. As can be noted from previous results, the temperature does not have a large impact on the outcome. However, in Figure 18 an interesting pattern is shown. This figure shows a stress test with on the x-axis a change in total mean precipitation and on the y-axis the change in extreme precipitation (P^{99}). Interesting here is to note that both variables play a role on the outcome of maximum daily discharges. So in terms of maximum daily discharge, P^{99} changes should be considered.

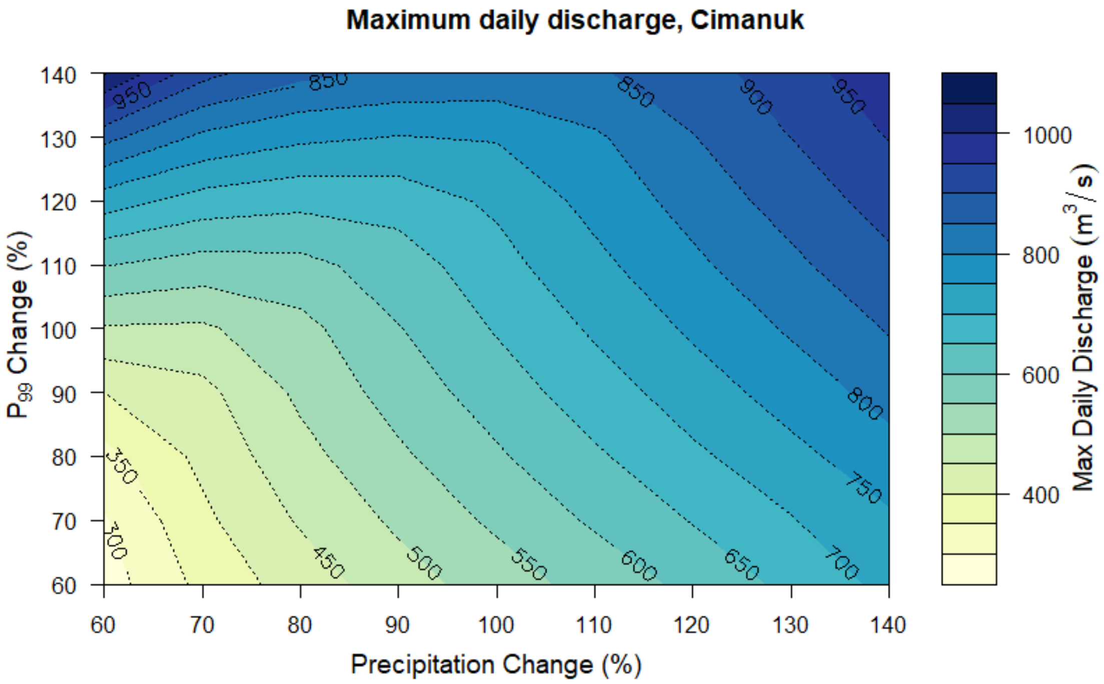

Figure 18 Stress test of the maximum daily discharge in the Cimanuk river, based on changes in temperature and precipitation.

6.2.3 GCMs average daily discharge

In order to show the likelihood of previous results, the projections of a large range of GCMs for four RCPs are plotted over previous maps to indicate the effect of climate change on the Cimanuk basin. However, only delta *P* (changes in annual precipitation sums) and delta *T* (changes in average temperature) were used in this study for the reference periods of 2030, 2050, and 2100.

First the results of all GCMs with different RCPs for 2030 are shown in Figure 19a. It shows that the precipitation change in 2030 is more uncertain than the temperature change. As explained before this means that also a large uncertainty is present regarding average daily discharges in 2030. These discharges can range from 90 m^3/s to 200 m^3/s.

In Figure 19b the results of 2050 are shown. The spread is increasing including the uncertainty. Though, it is noticed that the amount of precipitation change spreading is similar compared to 2030, but the temperature change spread is larger. As the temperature has minor impact on the average daily discharge the values of average discharge are similar to those of 2030.

Finally, in Figure 19c the results of 2100 are shown. Here, the spread of the GCM data is the largest for both precipitation (ranging from 65% to 130%) and temperature (ranging from 0 °C towards 4 °C). This means that the possible average daily discharge can range from 240 m^3/s to 55 m^3/s.

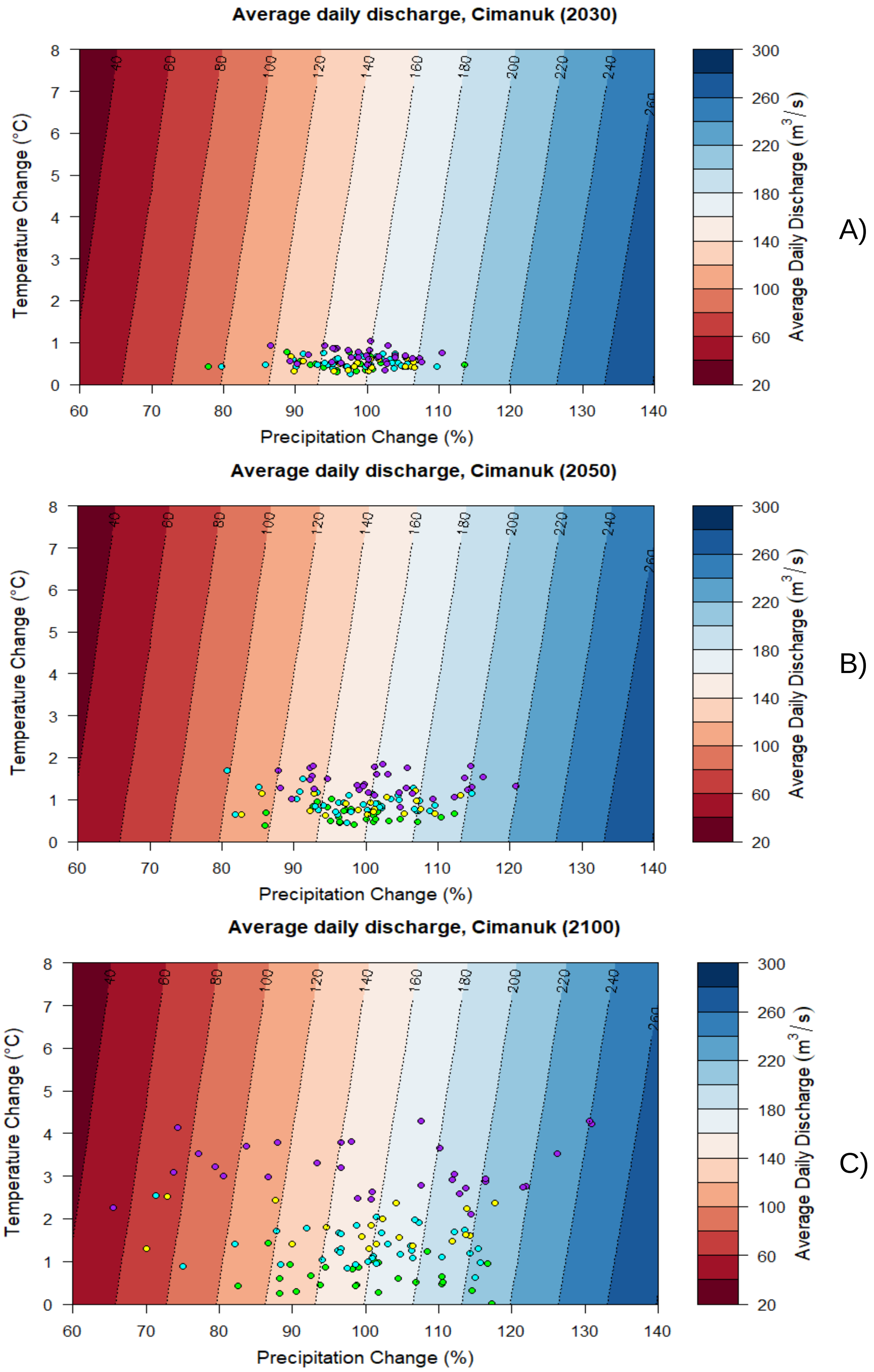

Figure 19 Outcome of the “Bottom-up” CRA approach for the average daily discharge in the Cimanuk river under changes in precipitation (x-axis) and temperature (y-axis). Colored circles represent mean climate change projections from a multi-model ensemble of GCMs (RCP2.6 – green; RCP4.5 – cyan; RCP6.0 – yellow; RCP8.5 – purple). Figure A, represents the projection for 2030; Figure B, represents the projection for 2050; Figure C, represents the projection for 2100.

6.2.4 *Future hydrological extremes*

As the spread of the GCMs of the different periods are shown previously, the same method can also be applied to the other maps. As we would like to know the effect of the most extreme outcome for future hydrological extremes, only the maps of 2100 for drought and maximum average daily discharge will be shown.

In terms of maximum discharge from Figure 20 it can be seen, again, that a large uncertainty is present. The GCMs are widely scattered and therefore climate change mitigation should keep in mind the possible outcomes. For maximum daily discharges the most extreme is based on the RCP8.5 providing a maximum daily discharge of almost 900 m^3/s. Contradictory the same RCP corresponds also to the lowest value corresponding to 325 m^3/s. Keep in mind that these values are based on daily averaged discharges and therefore higher discharges might be present.

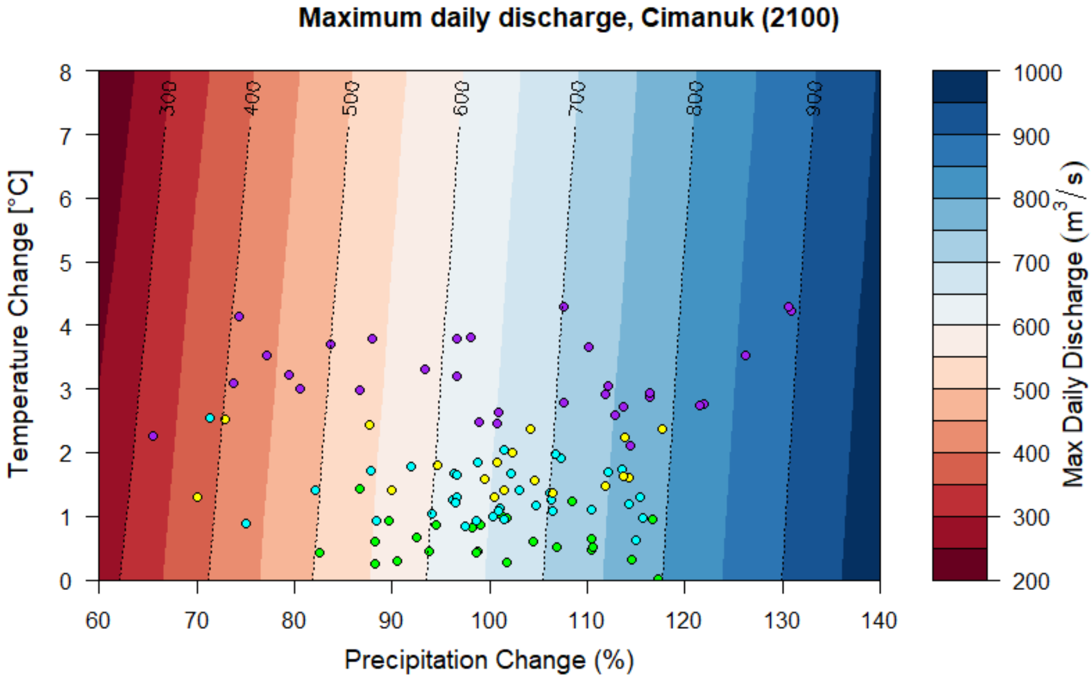

Figure 20 Outcome of the “Bottom-up” CRA approach, in 2100, for the maximum daily discharge of the Cimanuk river. Colored circles represent mean climate change projections from a multi-model ensemble of GCMs (RCP2.6 – green; RCP4.5 – cyan; RCP6.0 – yellow; RCP8.5 – purple).

Regarding low flows, the largest differences in terms of days below the 5th percentile are again caused by the same RCP8.5 (Figure 21). This indicates that there can become as much as 50 days below this threshold, or as few as 16.

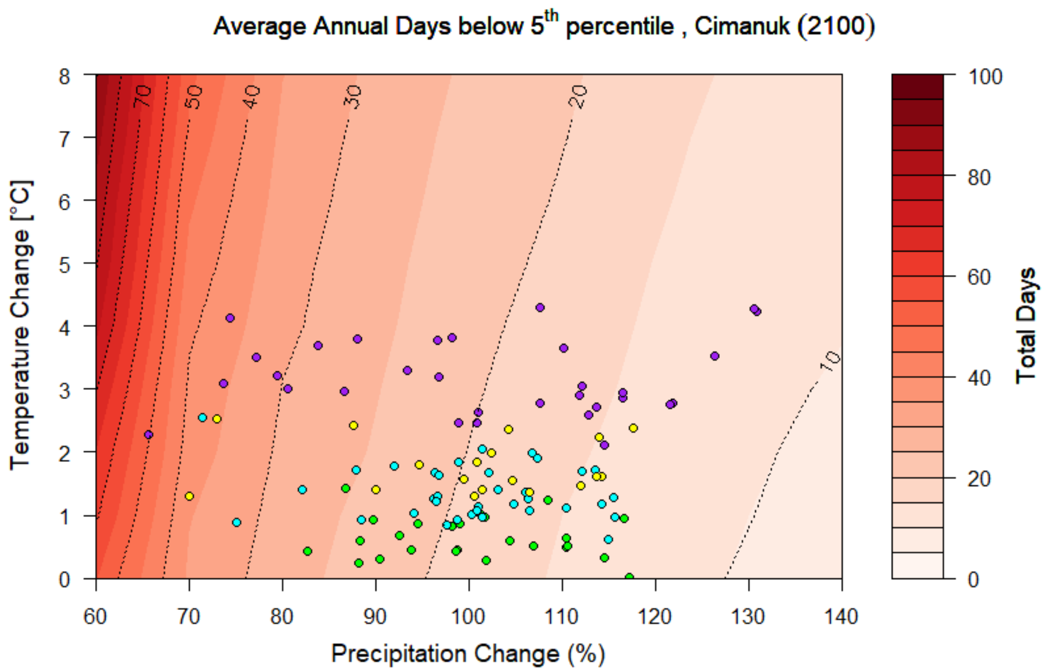

Figure 21 Outcome of the “Bottom-up” CRA approach, in 2100, for the average annual days below the 5th percentile discharge of the Cimanuk river. Colored circles represent mean climate change projections from a multi-model ensemble of GCMs (RCP2.6 – green; RCP4.5 – cyan; RCP6.0 – yellow; RCP8.5 – purple).

6.3 S. Cisanggarung

In order to analyze regional differences in the effects of climate change for hydrology, the same stress tests regarding mean discharge, maximum discharge, and days below the 5th percentile

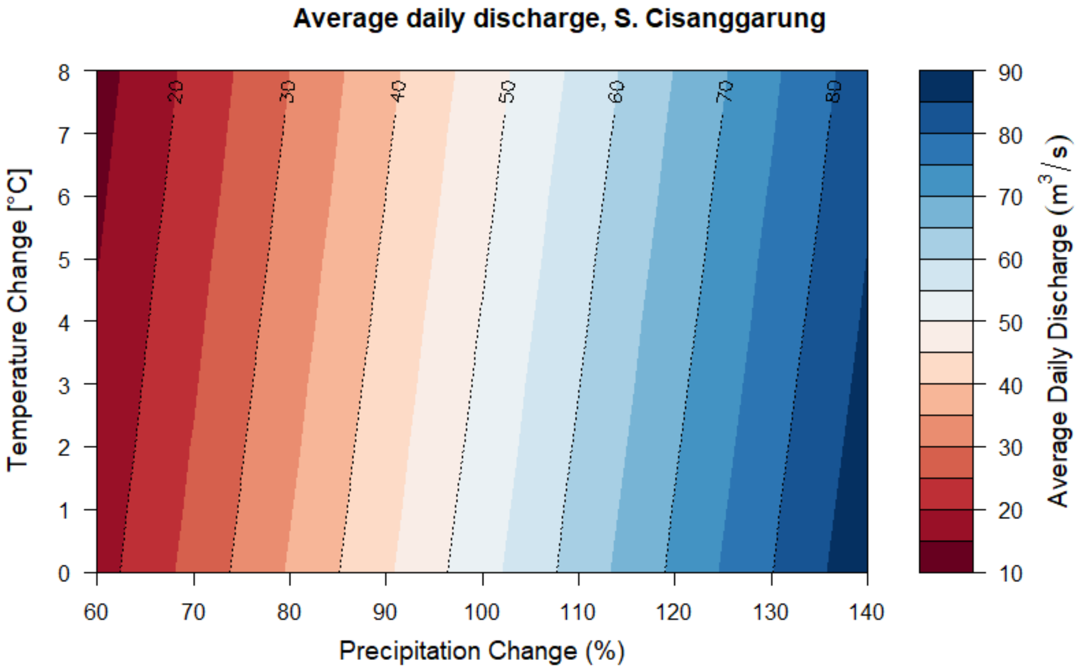

Figure 22 Stress test of the average daily discharge in the S. Cisanggarung river, based on changes in temperature and precipitation.

have been applied on a smaller basin. As seen before, the discharge pattern is little different compared to Cimanuk. However comparing Figure 22 with Figure 14 shows that the average discharge patterns is comparable.
However, as the area of these catchment are not similar, we should look at the percental changes to prove the identical pattern. In Figure 23 we see the same range of percental change as the stress test performed on Cimanuk and therefore we can say that there is barely any difference in terms of average daily discharge changes between a large and small sub-basin.

6.3.1 Future hydrological extremes

It is shown that the effect of climate change on the mean daily discharge is comparable to Cimanuk. In Figure 24 and Figure 25 hydrological extremes are shown. Here, the same stress tests are applied. First we analyzed the dry days, thus days under the threshold of the 5th percentile. Afterwards, another stress tests based on changes in P^{99} and P_{mean} was performed. Comparing these with the stress tests from Cimanuk indicates the same amount of dry days and the same pattern regarding maximum discharge. This indicates that the effect of climate change on this basin is identical to that of Cimanuk and that there is hardly any difference based on these results.

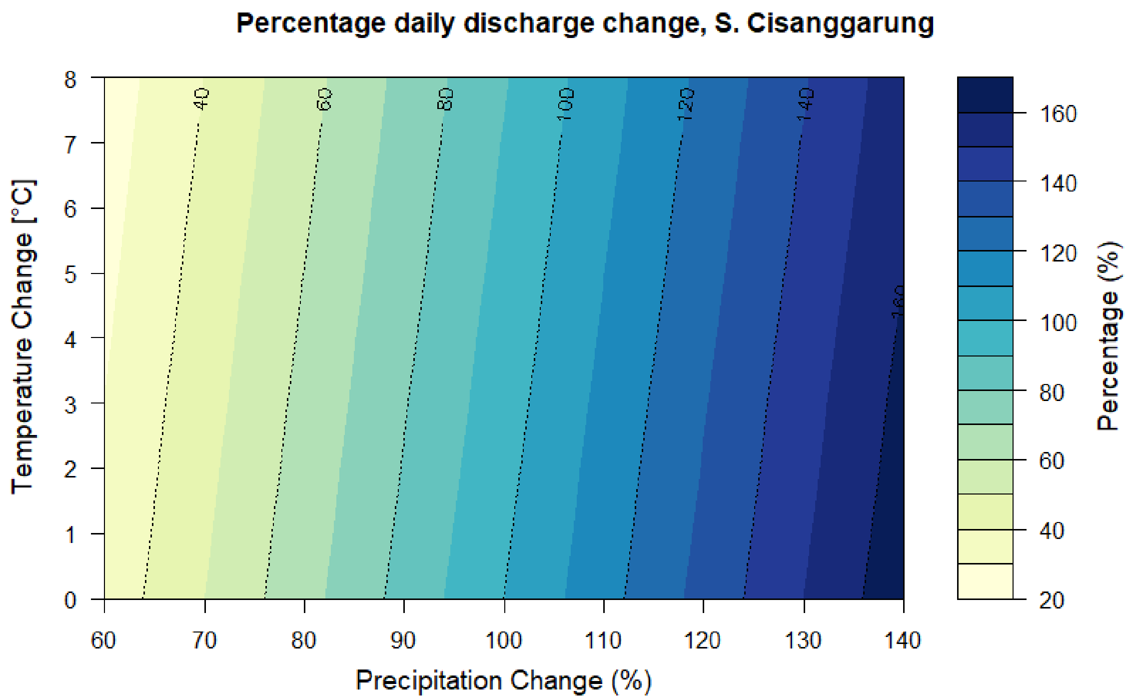

Figure 23 Percental change of average daily discharge in the S. Cisanggarung river, based on stress test with changes in temperature and precipitation

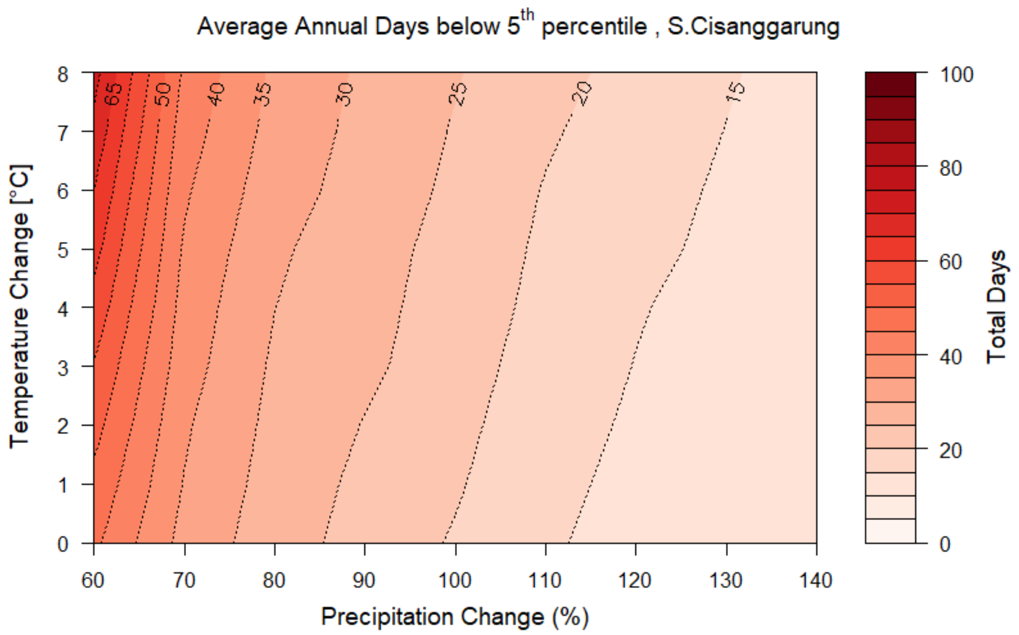

Figure 24 Stress test of the average annual days below the 5th percentile of discharge in the S. Cisanggarung river, based on changes in temperature and precipitation

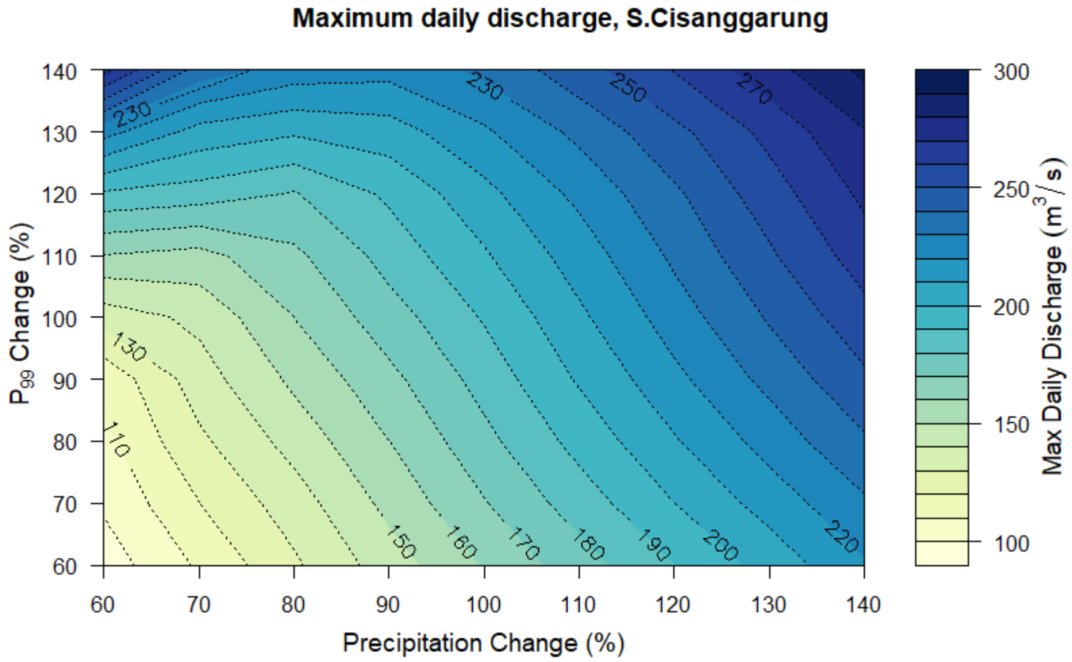

Figure 25 Stress test of the average daily discharge in the S. Cisanggarung river, based on changes in temperature and precipitation

7 Conclusions and Recommendations

The main objective was to study the impact of climate change on hydrological processes for the Cimanuk basin with the help of multiple research questions defined in section 1.2. Each section below is related to these research questions and provides an answer. At the end of this chapter the main research question is answered followed by a recommendations section.

7.1 Discharge stress test

SPHY has been used on the Cimanuk basin to model the discharge of all the main rivers in this basin. As the final goal is to describe the water availability of the Cimanuk catchment, the output of this study will used in another study where the water allocation/supply model WEAP will be used. Therefore, per sub-basin discharges are needed including the effect of climate change. To understand the effects of climate change in this catchment, the proposed **"Bottom-up"** method is used. This method starts in the vulnerability domain and puts less emphasis on the GCMs and will provide a clear overview of the possible effects of climate change on certain processes.
The outcome of this method for the Cimanuk river is shown in section 6.2. The stress test of temperature and precipitation indicate that for the chosen range of these variables the discharge could rise by 180% or even decrease to 20%.The first research question can also be answered from these findings, where the question is defined as:

1. *What is the impact of temperature on discharge?*

Based on the results it is clearly visible that the temperature has barely any effect on the discharge and that precipitation is the dominant variable. This indicates that precipitation is the main driver of discharge change. Therefore the effect of temperature on discharge is not significant, except for low flows.

7.2 Climate change projections

Different RCPs (RCP2.6, RCP4.5, RCP6.0, and RCP8.5) have been used in combination with multiple GCMs to indicate the scope of climate projections on the stress method used before. The output of these GCMs are set to 2030, 2050, and 2100 to indicate the range of temperature and precipitation of future projections. Placing this output on the stress maps gave an insight in the possible range of hydrological outputs for different future scenarios. It was shown that for the most distant scenario (2100) combined with RCP8.5 resulted in the most extreme output combined with the highest uncertainty. This output indicated for multiple hydrological variables (e.g. average daily discharge, highest daily discharge) both the lowest as well as the highest values. Therefore the second research question, defined as:

2. Will the climate projection of 2100, compared to 2030 and 2050, have the most impact on the discharge?

can be answered. The pattern shows indeed that the most extreme values are present for the year 2100, however both maximum as minimum values are present indicating a large uncertainty. Also, the scatter is the largest for 2100.

The conclusion of the third question, which is :

3. *What is the impact of climate change on hydrological extremes?*

Can also be answered by taken into account the scatter of all GCMs, but now for extreme hydrological variables only (maximum daily discharge, dry days). It follows that when indicating the most extreme possibilities, maximum daily discharge can reach as high as 900 m^3/s in the Cimanuk catchment. Keep in mind that this value is a daily average only; larger peaks within the day can be present. Additionally, the effect of P_{99} is noticeable on peak discharges and should be considered by applying the bottom-up method for hydrological extremes. The amount of dry days can be as high as 50 days, however the large uncertainty due to the scatter should be taken into account.

7.3 Sub-basin Comparison

Not only was the Cimanuk river taken into account to indicate the effect of climate change on the whole catchment, but also a smaller sub-basin with S. Cisanggerung as the main river. While the Cimanuk river covers almost the whole catchment, it is also important to know if the effects on smaller sub-basins are similar. The fourth question can therefore be answered, which is defined as:

4. Does the effect of climate change depend on the basin size?

The slope of the catchment is higher and the land use is not identical in all sub-basins. Analyzing the same figures created before, but instead now for the S. Cisanggerung river, shows almost identical results. In terms of discharge, the hydrograph is peakier, due to the smaller basin and steeper slope. This results in less storage and therefore a quicker run-off response. However, analyzing the effects of climate change on average daily discharge and hydrological extremes show very little effect, indicating that the effect of climate change is identical to the basin of the Cimanuk river.

7.4 Hydrological effects of climate change

Taking all previous sections into account the main question can be answered:

- *“What is the impact of climate change on the hydrological processes in the Cimanuk catchment?”*

In terms of discharge, the main question to be answered is what the expected precipitation pattern will be in the future. Based on the used GCMs and RCPs precipitation patterns for future scenarios are uncertain. Because we showed the importance of precipitation on discharge, this is a key variable to understand the exact effect of climate change on hydrological effects and water availability. In terms of hydrological extremes, precipitation is again the key variable for discharge.

7.5 Recommendations and Discussion

The study reveals that without a lot of data, SPHY is still a practical tool to assess climate change effect on a basin in Indonesia. However, uncertainty is present in terms of smaller temporal scales. The temporal resolution is here set to a day which indicates that extreme

discharge peaks lasting several hours cannot be modelled, while daily peak discharges can. Also, proper validation data was lacking indicating that proper calibration on discharge is neglected. Additional data would improve the quality of the outcome.
The stress test was performed only based on constant factors for the entire year, whereas in reality under climate change the changes will probably differ within the year/per season. Also only changes in temperature and mean precipitation amounts are considered. While for extreme discharge P^{99} should also be considered. Finally, if more budget and time was available GCMs could be downscaled to take seasonal changes into account.

In terms of results, some unexplained phenomena's occurred related to high discharges. In Figure 18 and Figure 25 a stress test is performed with mean precipitation and P^{99}. However, in the northwestern corner, lower mean precipitation amounts indicate higher discharges while the P^{99} is constant.

To analyses the differences in discharge between both catchment, we use a percental approach. However, a comparison with mm/day or mm/year between both catchments could also be useful.

As the "bottom-up" approach is a new method, not many studies have done this method yet. However, the CRA of the Jilin Yanji (Droogers, 2018) has done the same "bottom-up" approach and indicates the same effect on discharge related to the change in temperature and precipitation.

8 Bibliography

Allen, R. G., Pereira, L. S., Raes, D., & Smith, M. (1998). Crop evapotranspiration-Guidelines for computing crop water requirements-FAO Irrigation and drainage paper 56. *FAO, Rome*, *300*(9), D05109.

Asian Development Bank. (2016). *Indonesia Country Water Assessment*. Retrieved from www.adb.org

Bartholomeus, R. P., Witte, J. P. M., van Bodegom, P. M., van Dam, J. C., & Aerts, R. (2008). Critical soil conditions for oxygen stress to plant roots: Substituting the Feddes-function by a process-based model. *Journal of Hydrology*, *360*(1–4), 147–165. https://doi.org/10.1016/j.jhydrol.2008.07.029

Beck, H. E., Vergopolan, N., Pan, M., Levizzani, V., Van Dijk, A. I. J. M., Weedon, G. P., et al. (2017). Global-scale evaluation of 22 precipitation datasets using gauge observations and hydrological modeling. *Hydrology and Earth System Sciences*, *21*(12), 6201–6217. https://doi.org/10.5194/hess-21-6201-2017

de Boer, F. (2016). HiHydroSoil : A high resolution soil map of hydraulic properties (Version 1.2). *Report FutureWater: 134*, *31*(January), 1–32.

Burton, I., Huq, S., Lim, B., Pilifosova, O., & Schipper, E. L. (2002). From impacts assessment to adaptation priorities: The shaping of adaptation policy. *Climate Policy*, *2*(2–3), 145–159. https://doi.org/10.3763/cpol.2002.0217

Carter, T. R., Parry, M. L., Harasawa, H., & Nishioka, S. (1994). IPCC Technical Guidelines for Assessing Climate Change Impacts and Adaptations. *Radioative Forcing of Climate Change; Evaluation of the IPCC IS92 Emission Scenarios and the IPCC Guidelines for Nacional Greenshouse Gas Inventories*.

Droogers, P. (2018). Climate Risk Assessment: Jilin Yanji Low-Carbon Climate-Resilient Urban Development.

Droogers, P., & Allen, R. G. (2002). Estimating reference evapotranspiration under inaccurate data conditions. *Irrigation and Drainage Systems*, *16*(1), 33–45. https://doi.org/10.1023/A:1015508322413

Feddes, R. A. (1978). Simulation of field water use and crop yield. *Simulation of Plant Growth and Crop Production*, *Pudoc*(Wageningen), 194–209.

Funk, C., Peterson, P., Landsfeld, M., Pedreros, D., Verdin, J., Shukla, S., et al. (2015). The climate hazards infrared precipitation with stations - A new environmental record for monitoring extremes. *Scientific Data*, *2*, 150066. https://doi.org/10.1038/sdata.2015.66

García, L. E., Matthews, J. H., Rodriguez, D. J., Wijnen, M., DiFrancesco, K. N., & Ray, P. (2014). *Beyond Downscaling: A Bottom-Up Approach to Climate Adaptation for Water Resources Management*. *AGWA Report 01*. World Bank Group, Washington, DC. Retrieved from https://openknowledge.worldbank.org/handle/10986/21066

Guerschman, J. P., Van Dijk, A. I. J. M., Mattersdorf, G., Beringer, J., Hutley, L. B., Leuning, R., et al. (2009). Scaling of potential evapotranspiration with MODIS data reproduces flux observations and catchment water balance observations across Australia. *Journal of Hydrology*, *369*(1–2), 107–119. https://doi.org/10.1016/j.jhydrol.2009.02.013

Hack, J. (1957). Studies of longitudinal stream profiles in Virginia and Maryland. *USGS Professional Paper 249*, 97. Retrieved from https://books.google.nl/books?hl=nl&lr=&id=BMHMKaKYdl0C&oi=fnd&pg=PA47&dq=hack+stream+order&ots=w9SiAWO99r&sig=jhH9EJDW2AcIs69epF0aAyX_Sj8

Hu, G., & Jia, L. (2015). Monitoring of evapotranspiration in a semi-arid inland river basin by combining microwave and optical remote sensing observations. *Remote Sensing*, *7*(3), 3056–3087. https://doi.org/10.3390/rs70303056

Karssenberg, D., Burrough, P. A., & Sluiter, R. (2001). Review Article The PCRaster Software and Course Materials for Teaching Numerical Modelling in the Environmental Sciences. *Main*, *5*(2), 99–110.

Leander, R., & Buishand, T. A. (2007). Resampling of regional climate model output for the simulation of extreme river flows. *Journal of Hydrology*, *332*(3–4), 487–496. https://doi.org/10.1016/j.jhydrol.2006.08.006

Lehner, B., Verdin, K., & Jarvis, A. (2006). HydroSHEDS Technical Documentation, 1–27. Retrieved from http://hydrosheds.cr.usgs.gov

Martens, B., Miralles, D. G., Lievens, H., Van Der Schalie, R., De Jeu, R. A. M., Fernández-

Prieto, D., et al. (2017). GLEAM v3: Satellite-based land evaporation and root-zone soil moisture. *Geoscientific Model Development*, *10*(5), 1903–1925. https://doi.org/10.5194/gmd-10-1903-2017

Mecikalski, J. R., Diak, G. R., Anderson, M. C., & Norman, J. M. (1999). Estimating Fluxes on Continental Scales Using Remotely Sensed Data in an Atmospheric–Land Exchange Model. *Journal of Applied Meteorology*, *38*(9), 1352–1369. https://doi.org/10.1175/1520-0450(1999)038<1352:EFOCSU>2.0.CO;2

Moss, R. H., Edmonds, J. A., Hibbard, K. A., Manning, M. R., Rose, S. K., Van Vuuren, D. P., et al. (2010). The next generation of scenarios for climate change research and assessment. *Nature*, *463*. https://doi.org/10.1038/nature08823

Mu, Q., Heinsch, F. A., Zhao, M., & Running, S. W. (2007). Development of a global evapotranspiration algorithm based on MODIS and global meteorology data. *Remote Sensing of Environment*, *111*(4), 519–536. https://doi.org/10.1016/j.rse.2007.04.015

Mu, Q., Zhao, M., & Running, S. W. (2011). Improvements to a MODIS global terrestrial evapotranspiration algorithm. *Remote Sensing of Environment*, *115*(8), 1781–1800. https://doi.org/10.1016/j.rse.2011.02.019

Senay, G. B., Budde, M., Verdin, J. P., & Melesse, A. M. (2007). A coupled remote sensing and simplified surface energy balance approach to estimate actual evapotranspiration from irrigated fields. *Sensors*, *7*(6), 979–1000. https://doi.org/10.3390/s7060979

Shabalova, M. V., van Deursen, W. P. A., & Buishand, T. A. (2003). Assessing future discharge of the river Rhine using regional climate model integrations and a hydrological model. *Climate Research*, *23*(3), 233–246. https://doi.org/10.3354/cr023233

Su, Z. (2002). The Surface Energy Balance System (SEBS) for estimation of turbulent heat fluxes. *Hydrology and Earth System Sciences*, *6*(1), 85–100. https://doi.org/10.5194/hess-6-85-2002

Terink, W., Lutz, A. F., Simons, G. W. H., Immerzeel, W. W., & Droogers, P. (2015). SPHY v2. 0: Spatial Processes in HYdrology. *Geoscientific Model Development*, *8*(7), 2009.

van Vuuren, D. P., Edmonds, J., Kainuma, M., Riahi, K., Thomson, A., Hibbard, K., et al. (2011). The representative concentration pathways: An overview. *Climatic Change*, *109*(1), 5–31. https://doi.org/10.1007/s10584-011-0148-z

Weedon, G. P., Balsamo, G., Bellouin, N., Gomes, S., Best, M. J., & Viterbo, P. (2014). The WFDEI meteorological forcing data set: WATCH Forcing data methodology applied to ERA-Interim reanalysis data. *Water Resources Research*, *50*(9), 7505–7514. https://doi.org/10.1002/2014WR015638

Wilby, R. L., & Dessai, S. (2010). Robust adaptation to climate change. *Weather*, *65*(7), 180–185. https://doi.org/10.1002/wea.543